Journal of Functional Materials and Applied Engineering

Research Paper

Preparation and Electrochemical Performance of an Aqueous Polymer Electrolyte for Highly Stable Zinc-Ion Batteries

Winai Oskuei[1], Safin Shui[1], Ludmila Mittler[2,*]

[1] enter of Excellence on Agricultural Biotechnology: (AG BIO/PERDO-CHE), Bangkok 10900, Thailand
[2] Department of Materials Science and EngineeringNational University of Singapore. Block E3A #03-147 Engineering Drive 1, Singapore 117574, Singapore
*Corresponding author: lmittler@nus.edu.sg

Abstract. The electrochemical integrity of metallic zinc anodes in aqueous zinc-ion storage systems is fundamentally compromised by hydrogen evolution parasitism, oxidative corrosion, and dendritic morphogenesis—phenomena that collectively impede extended cycling stability and high-rate operational capability. In this investigation, an innovative polymeric electrolyte salt formulation (MS electrolyte) was architected to simultaneously modulate bulk electrolyte microstructure and anode-electrolyte interfacial chemistry through the dense functional group array and extended chain topology of poly(2-acrylamido-2-methylpropane sulfonic acid zinc). Successful synthesis of the polymer was confirmed by 1H NMR and FTIR spectroscopy, and the MS electrolyte was prepared by dissolving it in deionized water, with conventional 1 mol/L $ZnSO_4$ aqueous solution (ZS electrolyte) used as a control. Electrochemical characterization demonstrates that the MS electrolyte formulation effectively mitigates parasitic interfacial reactions and dendritic proliferation at the zinc metal anode. Symmetric Zn-Zn configurations achieved extended cycling stability exceeding 600 h under moderate current density (1 mA/cm^2 , 1 mAh/cm^2), while sustaining 90 h of stable operation under aggressive conditions (10 mA/cm^2 , 10 mAh/cm^2). Asymmetric Zn-Cu cells delivered a mean Coulombic efficiency of 99.3% across 300 charge-discharge cycles. Full Zn-I_2 cells retained 86.1% of initial capacity after 1000 cycles at 1 A/g. Post-mortem analyses encompassing scanning electron microscopy, scanning electrochemical microscopy, X-ray diffraction, and Tafel polarization corroborate the suppression of surface corrosion and secondary reactions by the MS electrolyte system. This investigation furnishes a viable paradigm for aqueous zinc-ion electrolyte engineering that simultaneously realizes diminished water activity, enhanced ionic transport, and exceptional interfacial robustness, yielding consequential guidance for advancing high-performance aqueous zinc-ion battery technology.

Keywords: *Cellulose; Polyvinyl alcohol;Ionic gel; High-voltage window; Integrated flexible supercapacitors*

Received on 15 Dec 2021, Accepted on 15 Apr 2022, Published on 28 Apr 2022

Copyright © 2022 Hermela Senk *et al*. licensed to JFMAE. This is an open access article distributed under the terms of the CC BY-NC-SA 4.0, which permits copying, redistributing, remixing, transformation, and building upon the material in any medium so long as the original work is properly cited.

1 Introduction

The accelerating transition toward a decarbonized global energy system has repositioned stationary electrochemical energy storage as a cornerstone technology for achieving carbon-peak and carbon-neutrality objectives. Driven by the urgent need to mitigate climate change, national strategies worldwide are prioritizing the large-scale integration of variable renewable energy sources—principally solar photovoltaic and wind power—into modern electricity grids [1]. However, the intrinsic intermittency, diurnal variability, and seasonal mismatch of these resources introduce profound challenges related to grid stability, frequency regulation, and reliable power dispatch. Electrochemical energy storage systems, owing to their rapid response characteristics, modular scalability, and high round-trip efficiency, have emerged as the most effective technological enabler for buffering renewable fluctuations, providing ancillary services, and shifting energy temporally to align supply with demand [2, 3]. Within this landscape, aqueous battery chemistries—especially those utilizing multivalent metal anodes—are attracting unprecedented attention due to their intrinsic safety, environmental benignity, and cost advantage over non-aqueous lithium-ion systems, which rely on flammable organic electrolytes and geographically concentrated critical minerals such as cobalt and nickel.

Among the diverse suite of aqueous energy storage platforms under active investigation, aqueous zinc-ion batteries (AZIBs) have ascended to a position of exceptional prominence. Metallic zinc, employed as the negative electrode, offers a compelling constellation of attributes: a high theoretical capacity (820 mAh g^{-1}), a moderately low reduction potential (−0.76 V vs. standard hydrogen electrode), natural abundance, and mature metallurgical infrastructure ensuring low raw-material costs [4 – 6]. Furthermore, divalent Zn^{2+} charge carriers enable fast interfacial kinetics in many host materials, while the use of mildly acidic, water-based electrolytes eliminates fire hazards and simplifies cell manufacturing. Collectively, these merits render AZIBs one of the most credible near-term alternatives to lithium-ion batteries for grid-scale stationary storage, where energy density requirements are less stringent than in consumer electronics or electric vehicles, but safety, cycle life, and levelized cost per kWh are decisive.

Despite these strategic advantages, the practical realization of high-performance, long-lifespan AZIBs remains impeded by persistent and interrelated degradation phenomena occurring at the zinc anode–electrolyte interface. Fundamentally, the standard electrode potential of the Zn/Zn^{2+} couple resides below that of the hydrogen evolution reaction (HER), rendering water thermodynamically unstable in direct contact with metallic zinc. During galvanostatic cycling, this thermodynamic predisposition manifests as continuous hydrogen evolution, particularly under high current densities or overpotentials, leading to electrolyte consumption, gas accumulation, and internal pressure buildup [7, 8]. Concurrently, the localized pH elevation accompanying HER promotes the precipitation of insulating zinc-based corrosion products—most notably zinc hydroxysulfates such as $Zn_4SO_4(OH)_6 \cdot xH_2O$—which form passivating surface layers that disrupt ionic conduction and exacerbate interfacial inhomogeneity. Beyond chemical corrosion, the electrodeposition dynamics of Zn^{2+} are inherently prone to spatial non-uniformity: uneven electric-field distribution, localized current-density hotspots, and stochastic nucleation sites drive the formation of mossy, fibrous, or dendritic zinc morphologies. Over prolonged cycling, these protuberant structures can propagate through the separator, culminating in internal short circuits, thermal runaway, or catastrophic cell failure. These coupled degradation pathways—hydrogen evolution, anode corrosion, and dendritic proliferation—collectively undermine coulombic efficiency, accelerate capacity fading, and impose severe constraints on the calendar life and operational reliability of AZIBs, constituting the principal bottleneck impeding commercial translation.

In response to these challenges, the battery research community has devised a multifaceted arsenal of mitigation strategies targeting different components of the cell architecture. Artificial interfacial coatings—ranging from inorganic oxides and carbonaceous layers to hybrid organic–inorganic films—aim to physically isolate the zinc anode from direct electrolyte contact while permitting facile Zn^{2+} transport [9, 10]. Structured current collectors, including three-dimensional porous foams and alloy-modified substrates, seek to redistribute local current density and accommodate volume changes during plating/stripping [11]. Parallel efforts have explored alternative anode materials, such as zinc alloys and composite anodes, to suppress side reactions through thermodynamic and kinetic stabilization [12]. While these electrode-centric approaches have yielded notable performance improvements, they frequently entail complex fabrication processes, increased manufacturing cost, or compromised specific capacity, limiting their industrial scalability.

In contrast, electrolyte engineering has emerged as the most versatile, cost-effective, and industrially compatible strategy for addressing zinc anode instability. By directly modulating the bulk solvation environment of Zn^{2+} and reshaping interfacial reaction pathways, electrolyte design can simultaneously suppress parasitic chemistry, regulate ion-transport kinetics, and stabilize electrode – electrolyte interphases without necessitating elaborate electrode modifications [13 – 15]. Classical approaches include increasing salt concentration to reduce free water activity, introducing co-solvents such as ethylene glycol or dimethyl sulfoxide to alter hydrogen-bonding networks, and incorporating functional additives—including surfactants, anions, and chelating agents—to adsorb onto the anode surface or modify the solvation sheath [16–18]. More recent innovations have focused on the design of novel zinc salts with tailored molecular structures. For instance, Du et al. [19] developed an amphiphilic zinc salt, $Zn(BBI)_2$, whose unique molecular architecture weakens water – water interactions and promotes the in situ formation of a robust, ion-conductive interphase, effectively suppressing HER and dendritic growth. Similarly, Chen et al. [20] engineered an asymmetric anionic zinc salt, $Zn(DFTFSI)_2$, which selectively adsorbs and reductively decomposes at the anode surface to generate a ZnF_2-rich solid electrolyte interphase, dramatically enhancing interfacial robustness.

Alongside molecular salt design, polymer-based aqueous electrolytes have gained considerable traction as a complementary strategy for enhancing both safety and cycling stability. Polymeric matrices—including polyvinyl alcohol, polyacrylamide, and cellulose derivatives—can physically immobilize water molecules, reduce electrolyte vapor pressure, and form quasi-solid or gel-like architectures that mechanically suppress dendrite propagation [21 – 23]. Moreover, judicious selection of functional groups enables polymers to coordinate with Zn^{2+}, modulate ion-solvation structures, and even serve as anion receptors or polyiodide traps in full-cell configurations. However, despite these conceptual advances, reports on rationally engineered functional polymers specifically tailored for AZIBs remain relatively scarce. Most existing polymer electrolytes prioritize mechanical integrity or ionic conductivity alone, without holistically addressing water activity suppression, Zn^{2+} desolvation kinetics, and interfacial electric-field homogenization. Consequently, the molecular-level structure – property relationships governing polymer – ion – water interactions in AZIBs are not yet fully elucidated, and the development of unified electrolyte systems capable of simultaneously delivering high ionic conductivity, suppressed side reactions, and dendrite-free cycling remains an outstanding scientific challenge.

Addressing this gap, the present investigation introduces an innovative macromolecular electrolyte architecture founded upon poly(2-acrylamido-2-methylpropane sulfonic acid zinc) (PAMPS-Zn). Leveraging the dense distribution of sulfonate functional groups and the extended conformational topology of the polymer backbone, this system is designed to exert simultaneous control over bulk electrolyte microstructure and zinc anode interfacial chemistry. Unlike conventional $ZnSO_4$ electrolytes—where free water molecules actively participate in parasitic reactions—the PAMPS-Zn polymer engages in strong coordinative interactions with both Zn^{2+} cations and H_2O molecules, restructuring the Zn^{2+} solvation sheath and reducing the chemical activity of bulk water. Simultaneously, the polymer scaffold homogenizes local electric-field distribution and Zn^{2+} flux during plating/stripping, eliminating nucleation hotspots that initiate dendritic growth. As demonstrated herein, symmetric Zn||Zn cells assembled with this polymeric electrolyte achieve exceptional cycling stability exceeding 600 hours, while Zn||Cu asymmetric cells deliver an average coulombic efficiency of 99.3% over 300 cycles. In full Zn–I_2 cells, the polymer electrolyte further suppresses polyiodide shuttling through electrostatic confinement, enabling 86.1% capacity retention after 1000 cycles. Collectively, this work furnishes a viable and scalable design paradigm for aqueous zinc-ion electrolyte engineering that harmoniously integrates diminished water activity, elevated ionic transport, and exceptional interfacial robustness—offering consequential guidance for advancing high-performance, long-lifespan AZIBs toward practical grid-scale deployment..

2. Experimental Materials and Methods

2.1 Material Preparation

AMPSZn Monomer Synthesis: Within a beaker containing 45 g deionized water, predetermined quantities of 2-acrylamido-2-methylpropane sulfonic acid and stoichiometric excess zinc hydroxide were introduced. The suspension was agitated for 1 h to ensure complete neutralization and salt formation. The resultant solution was subsequently transferred to centrifuge vessels and subjected to 1 h centrifugation to eliminate unreacted $Zn(OH)_2$, yielding a clarified AMPSZn stock solution.

MS Polymer Synthesis: To the clarified AMPSZn aqueous solution, VA-044 initiator (2.5 wt% relative to monomer mass) was introduced and homogenized under ambient conditions for 10 min. The reaction mixture was then transferred to a hermetically sealed vessel, subjected to 30 min high-purity nitrogen sparging, and thermally polymerized in a 50 °C oil bath for 24 h. Post-polymerization, the crude product underwent 3-day dialysis to exhaustively remove residual monomeric species. The purified material was subsequently vacuum-desiccated at 60 °C for 24 h, yielding the target poly(2-acrylamido-2-methylpropane sulfonic acid zinc) macromolecule.

2.2 Cathode Material Preparation

Iodine Cathode Preparation: AC@I_2 composites were synthesized via a conventional melt-diffusion method. Specifically, iodine and activated carbon were comminuted and intimately blended at 1:1 mass proportion, then sealed and thermally treated at 100 °C for 6 h. The resulting AC@I_2 composite was subsequently formulated into cathode ink by combining with polyvinylidene fluoride binder and conductive carbon black at 8:1:1 mass ratio.

This homogeneous dispersion was uniformly deposited onto carbon cloth substrates (12 mm diameter) and vacuum-desiccated at 60 °C for 6 h. The I_2 loading was controlled within the range of approximately 1.7–2 mg/cm^2.

2.3 Electrolyte Preparation

Stoichiometric zinc sulfate heptahydrate was dissolved in deionized water to formulate a 1 M $ZnSO_4$ aqueous electrolyte (designated ZS). Separately, the MS polymer was dispersed in deionized water to yield a polymeric electrolyte comprising 20 wt% MS (designated MS electrolyte), with mass fraction expressed relative to total electrolyte mass. Through actual solid content testing of the MS electrolyte, the measured average solid content was 19.8 ± 0.3 wt%.

2.4 Material Structure Characterization and Performance Testing

The synthesized polymer was dissolved in deuterated dimethyl sulfoxide for proton nuclear magnetic resonance characterization (^{1}H NMR, Bruker AVANCE III 400 MHz). Infrared vibrational spectra were acquired on a Thermo Scientific Nicolet 6700 spectrometer. Crystallographic phase identification of zinc anode surfaces was performed via X-ray diffraction (Bruker D8 Advance, Cu Kα, λ = 1.504 Å). Surface topographical characteristics were investigated through scanning electron microscopy and laser scanning confocal microscopy.

2.5 Electrochemical Performance Testing

CR2032 coin-type cells were fabricated using glass fiber separators and either 1 M $ZnSO_4$ or 20 wt% MS aqueous electrolytes, configured as Zn-Zn symmetric, Zn-Cu asymmetric, and Zn-I_2 full cell architectures. The cells were assembled sequentially from bottom to top with the negative case, zinc foil, glass fiber separator, 80 µL electrolyte, carbon cloth loaded with active material, spacer, spring, and positive case. Electrochemical characterization was performed on a Neware battery testing system (CT-4008T-5V50mA-164). Symmetric Zn-Zn cells underwent galvanostatic cycling across current densities of 1.0–10.0 mA/cm², with 1 h duration per half-cycle. Asymmetric Zn-Cu cells were evaluated for zinc plating/stripping Coulombic efficiency at 1 A/g with equivalent half-cycle duration. Electrochemical impedance spectroscopy, linear sweep voltammetry, and cyclic voltammetry measurements were conducted using a Bio-Logic electrochemical workstation. Scanning electrochemical microscopy (CHI-900D) was employed to probe localized electrochemical activity at the zinc anode surface.

3. Results and Discussion

3.1 Polymer Structure Characterization

The molecular architecture of the synthesized MS polymer was verified through proton nuclear magnetic resonance and Fourier-transform infrared spectroscopic analysis. As illustrated in Figure 1, the ^{1}H NMR spectrum exhibited characteristic resonance signals attributable to polymeric moieties, confirming successful chain propagation. The FTIR spectrum provided complementary validation, displaying diagnostic absorption bands associated with specific functional groups. Specifically, the broad feature at 3039 cm^{-1} was assigned to symmetric and asymmetric N–H stretching modes, the band at 1650 cm^{-1} corresponded to carbonyl stretching, and the sulfonate stretching vibration manifested near 1000 cm^{-1}. The presence of these characteristic peaks fully proves the successful synthesis of the MS polymer. Subsequently, the obtained polymer was dissolved in deionized water to prepare the corresponding macromolecular polymer electrolyte solution, hereafter referred to as MS electrolyte, for investigating its influence on zinc anode electrochemical stability, reversibility, and full-cell performance. The control group electrolyte was a conventional 1 mol/L zinc sulfate solution, hereafter referred to as ZS electrolyte. In contrast to the ZS electrolyte—which comprises a simple dissociated ionic system of unbound water molecules, zinc cations, and sulfate anions—the MS electrolyte features linear polymeric chains homogeneously distributed within the aqueous phase. These macromolecular backbones engage in coordinative interactions with zinc ions and water molecules, thereby reconfiguring the local solvation microenvironment surrounding zinc centers. This fundamental distinction in microscopic solvation architecture and interfacial interaction behavior between the two electrolyte formulations is systematically examined in subsequent sections regarding zinc anode electrochemical stability, zinc plating/stripping reversibility, and Zn-I_2 full cell cycling durability.

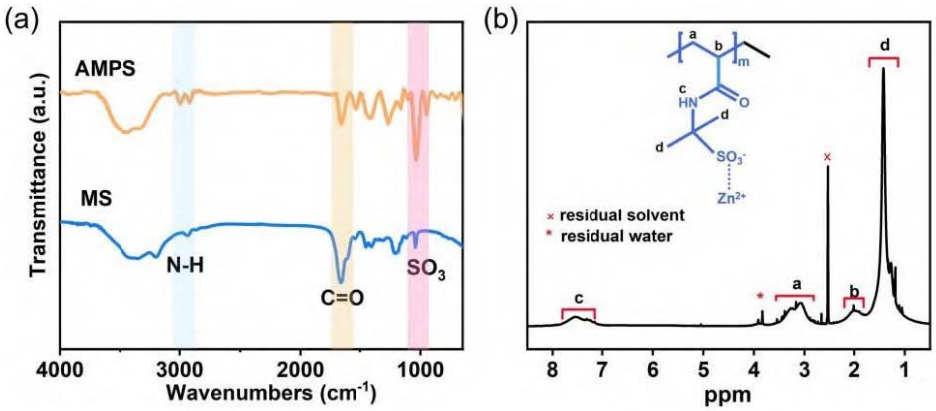

Figure 1 (a) FTIR spectra of the AMPS and MS polymer; (b) 1H NMR spectrum of the MS polymer

3.2 Inhibition of Zinc Anode Interfacial Dendrites and Side Reactions

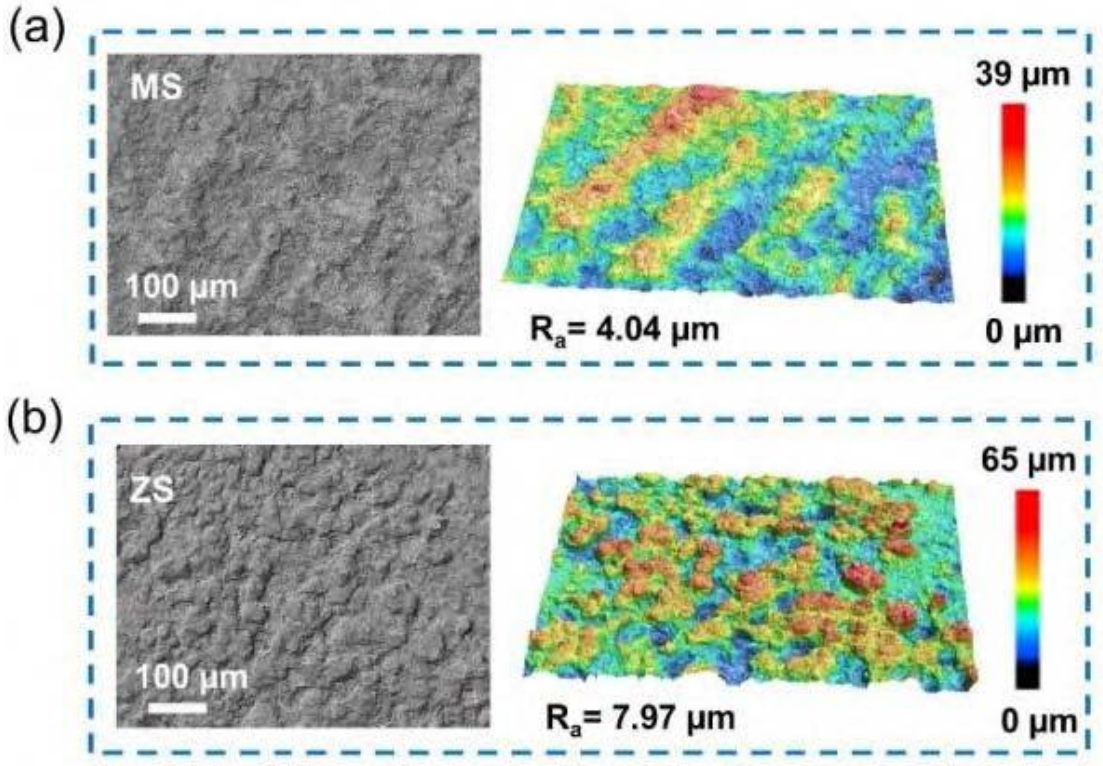

Figure 2 (a)~(b) SEM and LSCM images of zinc anodes after cycling in MS and ZS electrolytes

At the zinc anode-electrolyte boundary, dendritic morphogenesis and parasitic reactions (encompassing insoluble deposit formation and hydrogen evolution) invariably compromise the electrochemical integrity of the metallic zinc electrode. To evaluate the suppressive efficacy of the MS electrolyte formulation against dendritic proliferation and interfacial side processes, morphological evolution of cycled zinc surfaces was examined via scanning electron microscopy and laser scanning confocal microscopy. As depicted in Figure 2(a), the zinc electrode cycled in MS electrolyte presented a comparatively smooth, planar topography with minimal surface roughness (Ra = 4.04), signifying effective mitigation of both dendritic growth and parasitic interfacial chemistry. Conversely, the ZS electrolyte-cycled anode exhibited pronounced surface protrusions, irregular topographic features, dense disordered dendritic architectures, and byproduct accumulation [Figure 2(b)], accompanied by substantially elevated surface roughness (Ra = 7.97). These observations collectively demonstrate that the MS electrolyte facilitates homogeneous zinc electrodeposition while effectively suppressing dendrite nucleation and

interfacial side reactions.

X-ray diffraction was further deployed to characterize the crystalline phase assemblage of cycled zinc anode surfaces, corroborating the suppressive action of the MS electrolyte against interfacial parasitic chemistry. As illustrated in Figure 3(a), prominent diffraction signatures corresponding to zinc hydroxide sulfate hydrate [$Zn_4SO_4(OH)_6{\cdot}xH_2O$] were evident on the ZS electrolyte-cycled zinc surface, confirming substantial interfacial side reaction occurrence and byproduct accumulation during galvanostatic cycling. In marked contrast, the MS electrolyte-cycled anode exhibited complete absence of these diagnostic peaks, indicating effective inhibition of deleterious interfacial product formation and promotion of structurally stable zinc electrode architecture.

Tafel polarization analysis was conducted to further appraise anodic corrosion behavior across electrolyte formulations. As depicted in Figure 3(b), the MS system demonstrated elevated corrosion potential (0.025 V) and diminished corrosion current density (0.155 mA/cm²) relative to the ZS counterpart, signifying attenuated thermodynamic driving force and kinetic rate for oxidative degradation, respectively. Linear sweep voltammetry additionally illuminated the modulatory influence of MS electrolyte on interfacial parasitic processes [Figure 3(c)]. Hydrogen evolution was markedly suppressed, while oxygen evolution onset was anodically shifted (-0.148 V), collectively indicating expanded electrochemical stability domain. These findings confirm that the MS electrolyte effectively mitigates anodic corrosion, aqueous electrolyte decomposition, and byproduct accumulation, thereby substantially enhancing interfacial robustness.

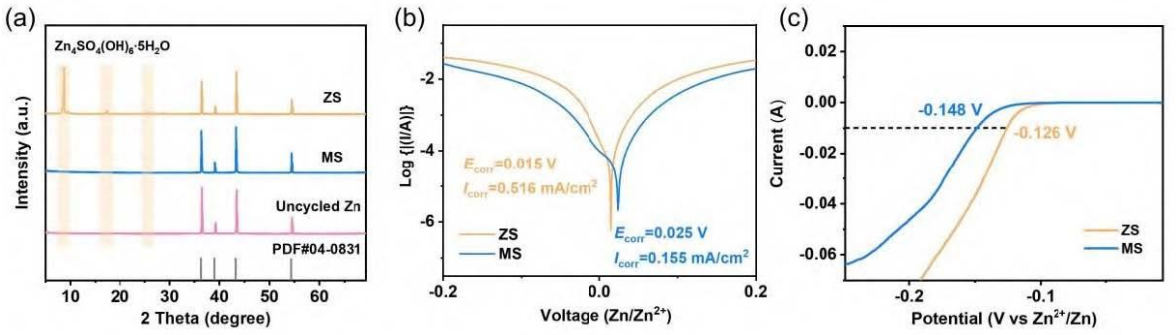

Figure 3 (a) XRD patterns of zinc anodes after cycling in ZS and MS electrolytes; (b) Tafel plots tested in ZS and MS electrolytes; (c) LSV curves of ZS and MS electrolytes

Scanning electrochemical microscopy (SECM) was utilized to further investigate the localized electrochemical behavior on the surface of the cycled zinc metal anode. Generally, electrochemically inert surfaces or those with limited electron transport exhibit negative feedback current responses ($i/i_{ss} < 1$), whereas highly conductive or electrochemically active surfaces tend to exhibit positive feedback current responses ($i/i_{ss} > 1$). Since zinc dendrites often originate from non-uniform local current density distribution and possess high conductivity, approaching dendritic-rich regions with the SECM probe typically yields significant positive feedback signals. As illustrated in Figures 4(a)–(b), the zinc electrode cycled in ZS electrolyte displayed pronounced spatial heterogeneity in localized current response, accompanied by positive feedback signatures indicative of substantial electrochemical activity disparities and significant dendritic proliferation. Conversely, the MS electrolyte-cycled anode predominantly exhibited uniform negative feedback characteristics with homogeneous current distribution, demonstrating that the polymeric electrolyte effectively modulates local electric field distribution during zinc electrodeposition, thereby suppressing dendrite preferential growth and fostering a more uniform, stable plating interface.

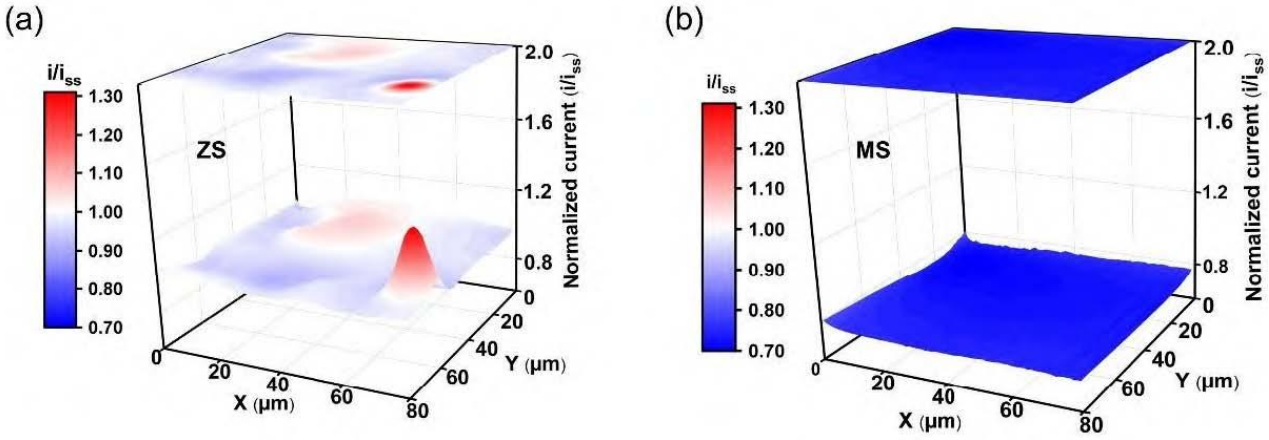

Figure 4 SECM images of zinc anodes after cycling in different electrolytes: (a) ZS (b) MS

3.3 Electrochemical Stability and Reversibility of Zinc Anode

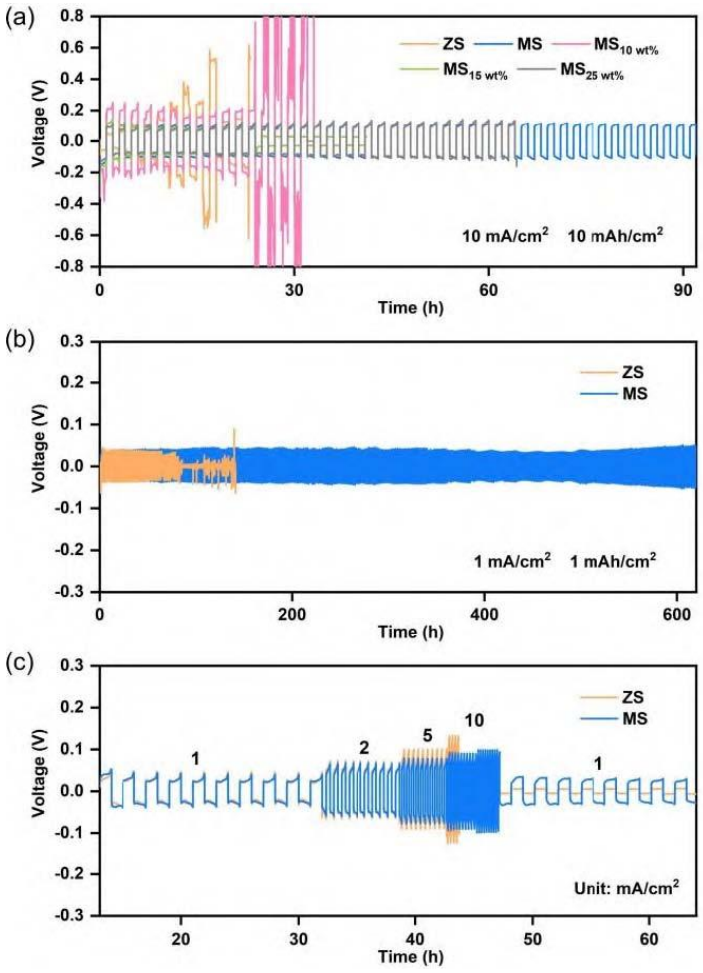

Figure 5 Long-term cycling tests of Zn-Zn batteries with ZS and MS electrolytes at different current densities: (a) 10 mA/cm2, (b) 1 mA/cm2; (c) Rate performance of Zn-Zn cells of ZS and MS at current densities of 1-10 mA/cm2

To identify the optimal polymer loading, gradient concentration screening was performed under aggressive cycling conditions (10 mA/cm², 10 mAh/cm²) [Figure 5(a)]. Comparative evaluation of symmetric cell longevity

and polarization stability across varying MS concentrations established 20 wt% as the favorable formulation. Leveraging this optimized composition, the regulatory influence on zinc metal anode electrochemical robustness and plating/stripping reversibility was systematically investigated. Under severe operating conditions, MS-equipped symmetric cells sustained 90 h of stable cycling, whereas ZS-based counterparts experienced rapid failure within approximately 10 h. Extended characterization under moderate conditions (1 mA/cm², 1 mAh/cm²) [Figure 5(b)] revealed ZS cells failing after merely 80 h with erratic polarization profiles, indicative of internal short-circuiting driven by dendritic bridging and interfacial byproduct accumulation. In marked contrast, MS-configured cells achieved exceptional cycling durability exceeding 600 h with stable overpotential, representing a sevenfold enhancement. Rate capability assessment across 1–10 mA/cm² at fixed 1 mAh/cm² areal capacity [Figure 5(c)] demonstrated that MS cells maintained stable voltage response throughout, while ZS cells exhibited severe polarization fluctuations at 10 mA/cm², confirming compromised structural integrity.

Zn-Cu asymmetric cells were assembled to further appraise zinc metal anode reversibility during plating/stripping across electrolyte formulations. As depicted in Figures 6(a)–(c), under moderate cycling conditions (1 mA/cm², 1 mAh/cm²), the ZS-configured cell demonstrated inferior cycling durability, failing within approximately 60 cycles accompanied by substantial voltage instability and depressed average Coulombic efficiency—attributable to aggravated dendritic morphogenesis and interfacial parasitic chemistry. Conversely, the MS electrolyte-enabled cell sustained 300 consecutive cycles (600 h) with regular, smooth galvanostatic profiles and exceptional average Coulombic efficiency of 99.3%. These findings collectively confirm that the MS electrolyte substantially enhances both electrochemical stability and deposition/stripping reversibility of the zinc metal negative electrode.

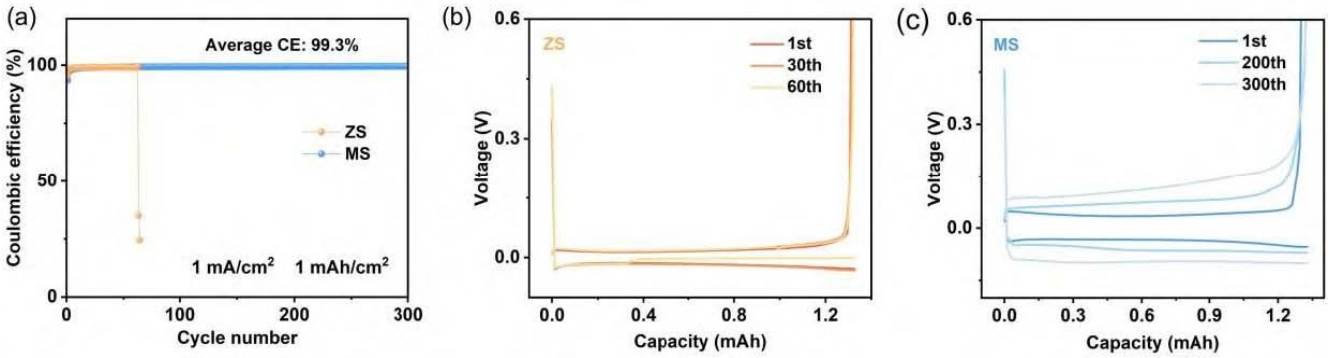

Figure 6 (a) Coulombic efficiency (CE) of Zn plating/stripping in Zn-Cu asymmetric cells; (b)~(c) Corresponding voltage profiles at various cycles

3.4 Electrochemical Performance of Zinc-Ion Batteries

To evaluate the practical viability of the MS electrolyte in full-cell configurations, Zn-I_2 complete cells were fabricated and subjected to comprehensive electrochemical characterization. Initially, reaction kinetics were probed via cyclic voltammetry at 1.0 mV/s [Figure 7(a)]. Both electrolyte systems exhibited characteristic redox couples corresponding to the I_2/I^- reversible conversion. Notably, the MS-configured cell demonstrated enhanced peak current densities with diminished peak potential separation, signifying accelerated electrochemical kinetics and elevated polysulfide redox activity. Electrochemical impedance spectroscopy [Figure 7(b)] corroborated these findings, revealing suppressed charge transfer resistance in the MS system relative to ZS. This indicates the polymeric electrolyte more effectively mediates interfacial charge transport, thereby facilitating polysulfide redox conversion dynamics. Therefore, the MS electrolyte effectively enhances the redox conversion kinetics of polysulfides in Zn-I_2 full cells, laying the foundation for its excellent cycling stability.

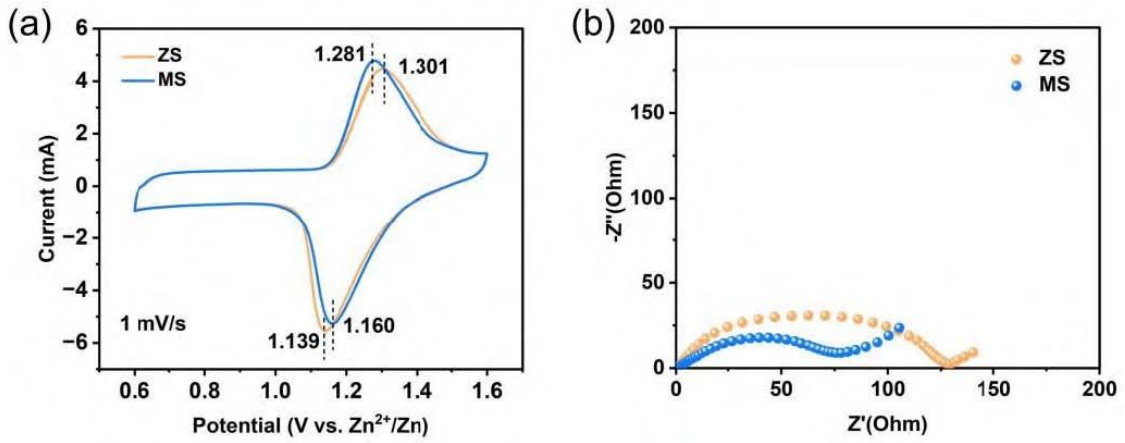

Figure 7 (a) CV curves of ZS and MS; (b) EIS spectra of ZS and MS

Self-discharge characteristics constitute a critical metric for assessing the practical viability of aqueous zinc-ion storage systems, fundamentally reflecting the chemical robustness and energy retention performance under open-circuit conditions. Elevated concentrations of highly reactive unbound water molecules in aqueous electrolytes readily induce persistent anodic corrosion and hydrogen evolution, while polyiodide species exhibit propensity for shuttle migration toward the negative electrode, collectively driving active material depletion and capacity deterioration during quiescent periods. Therefore, excellent self-discharge inhibition relies on a stable electrode/electrolyte interface and effective suppression of polyiodide shuttling migration. As depicted in Figures 8(a)–(b), the Zn-I_2 cell employing the MS electrolyte retained 83% Coulombic efficiency following 24 h open-circuit stand, substantially surpassing the 78% retention observed for the ZS-configured counterpart. This disparity substantiates the superior efficacy of the MS electrolyte in suppressing parasitic interfacial chemistry at the zinc anode and enhancing overall cell stability during quiescent operation. Further mechanistic analysis suggests that uniformly dispersed polymer chains in the MS electrolyte can adsorb and confine polyiodide ions such as I^{3-} and I^{5-} through intermolecular forces, forming a physical barrier effect that increases the diffusion resistance of polyiodides, effectively slowing their migration and shuttling toward the zinc anode, and synergistically inhibiting self-discharge behavior at the source.

The core mechanism underlying the performance enhancement originates from the unique molecular architecture of poly(2-acrylamido-2-methylpropane sulfonic acid zinc) (PAMPS-Zn), which fundamentally reconfigures the solvation microenvironment of zinc ions. Unlike conventional $ZnSO_4$ electrolytes where free water molecules actively participate in parasitic reactions, the densely distributed sulfonate groups and extended polymer chains in the MS electrolyte establish strong coordination interactions with both Zn^{2+} cations and H_2O molecules. This coordination network effectively reduces the chemical activity of bulk water, disrupting the hydrogen-bonding structure of the solvent and restricting the mobility of reactive species. By reconstructing the Zn^{2+} solvation sheath to replace free water molecules with polymer-bound functional groups, the electrolyte suppresses the thermodynamic tendency for hydrogen evolution and minimizes the availability of water for hydrolytic side reactions at the anode interface.

Interfacial stabilization is achieved through the synergistic regulation of electric field distribution and ion transport kinetics at the zinc anode surface. The polymer backbone acts as a three-dimensional scaffold that homogenizes Zn^{2+} flux during plating/stripping processes, eliminating localized current density spikes that typically nucleate dendritic growth. Scanning electrochemical microscopy confirms this effect, showing uniform negative feedback signals on MS-cycled anodes versus heterogeneous positive feedback (indicating dendrites) in control samples. Additionally, the polymer chains physically adsorb and confine corrosive intermediates—such as polyiodides in Zn-I_2 full cells—through electrostatic interactions and steric hindrance. This dual functionality prevents anode corrosion and inhibits the shuttle effect simultaneously, as evidenced by the absence of $Zn_4SO_4(OH)_6{\cdot}xH_2O$ byproducts in XRD analysis and the elevated corrosion potential in Tafel tests.

The integrated bulk-interfacial modulation translates into exceptional macroscopic electrochemical performance.

Symmetric cells achieve a 7-fold increase in cycling lifespan (600 h vs. 80 h) under moderate current densities due to suppressed dendrite penetration and reduced polarization. The Coulombic efficiency of Zn-Cu asymmetric cells reaches 99.3% over 300 cycles, reflecting highly reversible plating/stripping chemistry. In full Zn-I_2 cells, the polymer electrolyte accelerates redox kinetics—evidenced by lower charge transfer resistance in EIS and sharper CV peaks—while enhancing capacity retention to 86.1% after 1000 cycles. Crucially, the confinement of polyiodide species and stabilized anode interface reduce self-discharge, retaining 83% Coulombic efficiency after 24 h rest versus 78% for conventional electrolytes. This multifunctional design paradigm demonstrates that strategic polymer engineering can simultaneously address water reactivity, ion transport, and interfacial stability challenges in aqueous zinc-ion batteries.

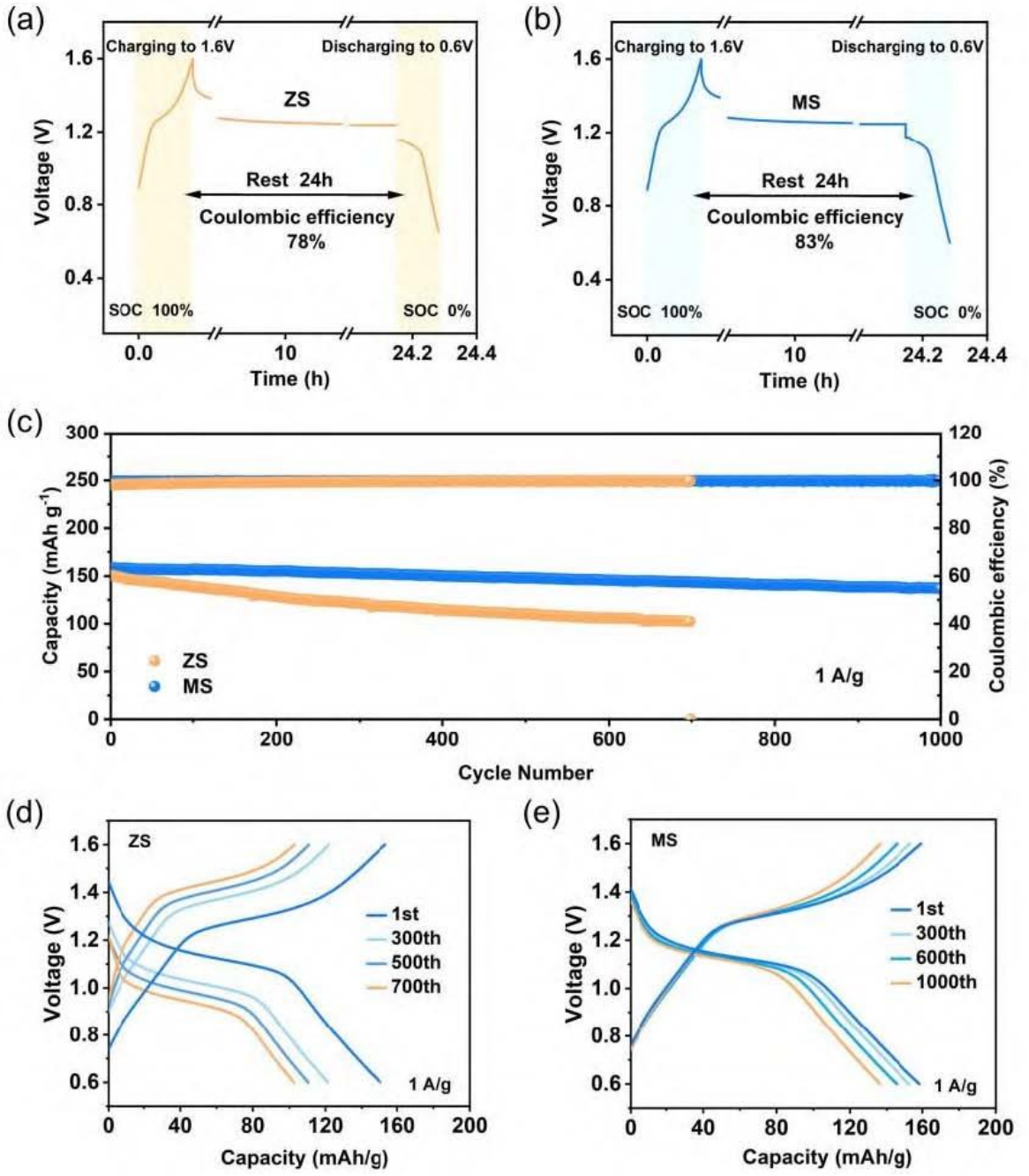

Figure 8 Self-discharge profiles of Zn-I2 batteries with (a) ZS and (b) MS electrolytes; (c) Long-term cycling performance of Zn-I2 batteries with ZS and MS electrolytes; Charge-discharge curves of the Zn-I2 battery using (d) ZS and (e) MS electrolytes

This work establishes a polymer-electrolyte design strategy that directly tackles the core failure mechanisms of aqueous zinc-ion batteries—hydrogen evolution, anode corrosion, and dendritic growth—through molecular-level modulation of the Zn^{2+} solvation environment. By synthesizing poly(2-acrylamido-2-methylpropane sulfonic acid zinc) (PAMPS-Zn) and formulating a 20 wt% aqueous MS electrolyte, the study demonstrates that densely distributed sulfonate groups and extended polymer chains cooperatively reduce bulk water activity, disrupt the hydrogen-bonding network, and reconstruct the Zn^{2+} solvation sheath. This structural reconfiguration suppresses thermodynamic drivers of parasitic reactions, as confirmed by Tafel polarization (higher corrosion potential, lower corrosion current) and linear sweep voltammetry (suppressed hydrogen evolution, expanded electrochemical stability window). Crucially, the polymer backbone functions as a three-dimensional scaffold that homogenizes local electric fields and Zn^{2+} flux during plating/stripping, eliminating current-density hotspots that initiate dendrites. Morphological and spectroscopic evidence—smooth anode surfaces (Ra = 4.04), absent $Zn_4SO_4(OH)_6 \cdot xH_2O$ byproducts in XRD, and uniform negative-feedback SECM signals—collectively validate the interfacial stabilization efficacy. Compared to prior electrolyte strategies such as high-concentration salts or small-molecule additives, this macromolecular approach offers a scalable, cost-effective route to simultaneously enhance bulk ionic transport, anode reversibility, and interfacial robustness without relying on toxic solvents or complex coating processes.

Electrochemical performance metrics underscore the practical utility of the MS electrolyte across device configurations. Symmetric Zn||Zn cells achieve a sevenfold lifespan extension (600 h vs. 80 h at 1 mA cm^{-2}) and sustain 90 h under aggressive 10 mA cm^{-2} /10 mAh cm^{-2} cycling, far outperforming conventional $ZnSO_4$ systems. Zn||Cu asymmetric cells deliver 99.3% average Coulombic efficiency over 300 cycles, reflecting near-ideal plating/stripping reversibility. In full Zn – I_2 cells, the polymer electrolyte not only improves redox kinetics—evidenced by sharper CV peaks and lower charge-transfer resistance—but also mitigates polyiodide shuttling via electrostatic confinement, boosting capacity retention to 86.1% after 1000 cycles and elevating 24 h self-discharge Coulombic efficiency to 83%. While the study focuses on iodine cathodes, the universal solvation-regulation mechanism suggests broad compatibility with other zinc-storage chemistries, such as MnO_2 or organic cathodes. Future work should explore mechanical reinforcement to prevent polymer creep under long-term cycling, as well as low-temperature performance and scale-up feasibility. Overall, this investigation provides a versatile materials paradigm for aqueous zinc batteries, aligning high safety, extended cycle life, and manufacturing practicality for grid-scale energy storage applications.

4. Conclusion

A macromolecular electrolyte architecture based on poly(2-acrylamido-2-methylpropane sulfonic acid zinc) was engineered, effectively suppressing parasitic interfacial chemistry and dendritic proliferation at the zinc metal anode while substantially enhancing electrochemical stability and plating/stripping reversibility. Symmetric Zn-Zn configurations achieved extended cycling durability exceeding 600 h under moderate conditions (1 mA/cm^2, 1 mAh/cm^2), with 90 h stability maintained under aggressive operating parameters (10 mA/cm^2, 10 mAh/cm^2). Asymmetric Zn-Cu cells demonstrated exceptional reversibility with 99.3% average Coulombic efficiency across 300 cycles. Full Zn-I_2 cells sustained 1000 cycles at 1 A/g with 86.1% capacity retention. This investigation furnishes a viable paradigm for aqueous zinc-ion electrolyte design integrating attenuated water activity, elevated ionic transport, and robust interfacial stability.

References

[1] ZAMPARDI G, LA MANTIA F. Open challenges and good experimental practices in the research field of aqueous Zn-ion batteries[J]. Nature Communications, 2022, 13(1): 687.

[2] LIU S, ZHANG R, WANG C, et al. Zinc ion Batteries: Bridging the Gap from Academia to Industry for Grid-Scale Energy Storage[J]. Angewandte Chemie International Edition, 2021, 63(17): e202400045.

[3] YU Y, XU W, LIU X, LU X. Challenges and Strategies for Constructing Highly Reversible Zinc Anodes in Aqueous Zinc-Ion Batteries: Recent Progress and Future Perspectives[J]. Advanced Sustainable Systems, 2020, 4(9): 2000082.

[4] TANG M, LIU Q, ZOU X, et al. High-Energy-Density Aqueous Zinc-Ion Batteries: Recent Progress, Design Strategies, Challenges, and Perspectives[J]. Advanced Materials, 2021, 37(48): 2501361.

[5] CHEN Y, YANG X, LI Y, et al. Mechanism and Application of Electrolyte Additives in Regulating Stability of Zinc Anode Interface in Aqueous Zinc Metal Batteries[J]. Advanced Functional Materials, 2020: e31039.
[6] LI Z, GUO J, CHANG L, et al. Engineering Trace-Amount Electrolyte Additives for Aqueous Zinc Batteries[J]. Advanced Energy Materials, 2021: e70899.
[7] YANG W, YANG Y, YANG H, ZHOU H. Regulating Water Activity for Rechargeable Zinc-Ion Batteries: Progress and Perspective[J]. ACS Energy Letters, 2020, 7(8): 2515-2530.
[8] CHEN M H, XIE S A, ZHAO X Y, et al. Aqueous zinc-ion batteries at extreme temperature: Mechanisms, challenges, and strategies[J]. Energy Storage Materials, 2022, 51: 683-718.
[9] PIAO Z, GAO R, LIU Y, et al. A review on regulating Li+solvation structures in carbonate electrolytes for lithium metal batteries[J]. Advanced Materials, 2022: e2206009.
[10] LI R, DU Y, LI Y, et al. Alloying Strategy for High-Performance Zinc Metal Anodes[J]. ACS Energy Letters, 2022: 457-476.
[11] ZHOU X, ZHOU Y, YU L, et al. Gel polymer electrolytes for rechargeable batteries toward wide-temperature applications[J]. Chemical Society Reviews, 2021, 53(10): 5291-5337.
[12] ZHANG N, HUANG S, YUAN Z, et al. Direct Self-Assembly of MXene on Zn Anodes for Dendrite-Free Aqueous Zinc-Ion Batteries[J]. Angewandte Chemie International Edition, 2021, 60(6): 2861-2865.
[13] CAO Q, GAO Y, PU J, et al. Gradient design of imprinted anode for stable Zn-ion batteries[J]. Nature Communications, 2020, 14(1).
[14] WANG Y, LIANG B, LI D, et al. Hydrogel electrolyte design for long-lifespan aqueous zinc batteries to realize a 99% Coulombic efficiency at 90℃[J]. Joule, 2021, 9(6): 101944.
[15] WANG C, ZENG X, QU J, et al. Salt-tolerance training enabled flexible molten hydrate gel electrolytes for energy-dense and stable zinc storage[J]. Matter, 2020, 6(11): 3993-4012.
[16] ZHANG Z, LAN X, LIAO G, et al. Coupling Zn2+Ferrying Effect With Anion-π Interaction to Mitigate Space Charge Layer Enables Ultra-High Utilization Rate Zn Anode[J]. Angewandte Chemie International Edition, 2020, 64(23): e202503396.
[17] WEI S, SHOU H, QI Z-H, et al. In situ Detection of the Molecule-Crowded Aqueous Electrode-Electrolyte Interface[J]. Journal of the American Chemical Society, 2021, 147(13): 10943-10953.
[18] WANG J, YANG Y, WANG Y, et al. Working Aqueous Zn Metal Batteries at 100℃[J]. ACS Nano, 2020, 16(10): 15770-15778. DOI:10.1021/acsnano.2c04114
[19] XIONG P, KANG Y, YAO N, et al. Zn-Ion Transporting, In Situ Formed Robust Solid Electrolyte Interphase for Stable Zinc Metal Anodes over a Wide Temperature Range[J]. ACS Energy Letters, 2021, 8(3): 1613-1625.
[20] WU X, XU Y, ZHANG C, et al. Reverse Dual-ion Battery via a ZnCl2 Water-in-Salt Electrolyte[J]. Journal of the American Chemical Society, 2019, 141(15): 6338-6344.
[21] WANG F, BORODIN O, GAO T, et al. Highly reversible zinc metal anode for aqueous batteries[J]. Nature Materials, 2018, 17(6): 543-549.
[22] ZHANG Q, MA Y, LU Y, et al. Modulating electrolyte structure for ultralow temperature aqueous zinc batteries[J]. Nature Communications, 2020, 11(1): 4463.
[23] JIANG H, TANG L, FU Y, et al. Chloride electrolyte enabled practical zinc metal battery with a near-unity Coulombic efficiency[J]. Nature Sustainability, 2021, 6(7): 806-815.
[24] DU H, DONG Y, LI Q J, et al. A New Zinc Salt Chemistry for Aqueous Zinc-Metal Batteries[J]. Advanced Materials, 2020, 35(25): 2210055.
[25] CHEN M, et al. An Asymmetric Anion Zinc Salt for Aqueous Zinc Metal Batteries[J]. Angewandte Chemie International Edition, 2021, 63(11): 202319125.